

LETTERS

PACS numbers: 42.55.Wd; 42.60.Lh; 32.50.+d
DOI: 10.1070/QE2011v041n07ABEH014668

Bismuth-doped germanosilicate fibre laser with 20-W output power at 1460 nm

S.V. Firstov, A.V. Shubin, V.F. Khopin, M. A. Mel'kumov,
I.A. Bufetov, O.I. Medvedkov, A.N. Gur'yanov, E.M. Dianov

***Abstract*. We report the first cw bismuth – germanium co-doped silica fibre laser with an output power above 20 W at 1460 nm and 50 % optical efficiency. The laser operates on a transition between energy levels of bismuth-related active centres associated with silicon. The incorporation of a small amount ($\sim$ 5 mol %) of germanium into the core of bismuth-doped silica fibre has little effect on its luminescence spectrum but reduces optical losses, which limit the laser efficiency.**

Keywords: *bismuth, fibre laser, bismuth-doped optical fibre*.

Bismuth-doped fibre lasers are capable of emitting between 1150 and 1550 nm (see the recent review by Bufetov and Dianov [1] and references therein). This wavelength range lies between the gain bands of ytterbium and erbium fibre lasers, which determines potential applications of the bismuth fibre lasers. CW bismuth fibre lasers operating at 1160, 1270 and 1330 nm with $\sim$ 10-W output power have been demonstrated in recent work [2 – 4]. The output power of the bismuth fibre lasers operating at longer wavelengths (1400 – 1500 nm) has not yet exceeded 2 W [4]. In this paper, we report a high-power efficient bismuth-doped fibre laser operating near 1460 nm. Some preliminary results were presented earlier [5].

The strongest luminescence band (near 1400 nm) is offered by bismuth-doped silica glass (BSG) and bismuth-doped germanosilicate glass (BGSG) fibres. In view of this, the properties of BSG fibre fabricated using the powder-in-tube technique and characterised earlier [6] are compared here to those of BGSG fibre fabricated using the MCVD process. The two fibres were drawn out from preforms at $T \approx 2000\,^{\circ}$C and were 125 μm in diameter. The bismuth content of the fibres did not exceed the detection limit of our analytical equipment (0.02 at %). Figure 1 shows grey-scale contours of the luminescence intensity, $I_{\rm lum}$, as a function of excitation and emission wavelengths ($\lambda_{\rm ex}$ and $\lambda_{\rm em}$) in the range 450 – 1600 nm for these fibres. The data were obtained under conditions similar to those described previously [6]. The luminescence peaks A, A1, A2, B and B1 in Fig. 1a are due to IR-emitting bismuth-related active centres (BACs), whereas peak C arises from Bi^{2+} [7 – 9].

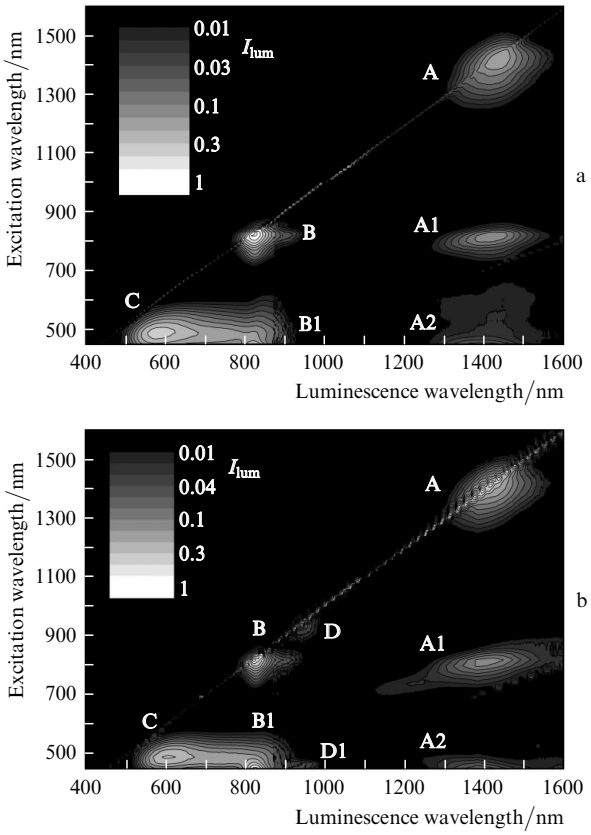

Figure 1. Grey-scale contours of $I_{\rm lum}(\lambda_{\rm em}, \lambda_{\rm ex})$ for the (a) BSG [6] and (b) BGSG fibres.

The luminescence spectrum of the BGSG (5 mol % GeO_2) fibre (Fig. 1b) differs only slightly from that of the BSG fibre: in addition to the peaks in Fig. 1a, the spectrum of the BGSG fibre contains peaks D ($\lambda_{\rm ex}^{\rm max} =$ 925 nm, $\lambda_{\rm em}^{\rm max} = 955$ nm) and D1 (460 nm, 955 nm) (Fig. 1b). Here, $\lambda_{\rm ex}^{\rm max}$ and $\lambda_{\rm em}^{\rm max}$ are the peak emission and peak excitation wavelengths, respectively. Peaks D and D1 are assignable to a new type of bismuth-related active centre, due to the presence of germanium in the BGSG fibre.

S.V. Firstov, A.V. Shubin, M. A. Mel'kumov, I.A. Bufetov, O.I. Medvedkov, E.M. Dianov Fiber Optics Research Center, Russian Academy of Sciences, ul. Vavilova 38, 119333 Moscow, Russia; e-mail: shubin@fo.gpi.ru, iabuf@fo.gpi.ru;
V.F. Khopin, A.N. Gur'yanov Institute of Chemistry of High-Purity Substances, Russian Academy of Sciences, ul. Tropinina 49, 603600 Nizhnii Novgorod, Russia

Received 15 June 2011
Kvantovaya Elektronika **41** (7) 581 – 583 (2011)
Translated by O.M. Tsarev

The optical properties of BACs in core glass are influenced not only by the glass composition but also by the redox properties of the glass, the (reducing or oxidising) gaseous atmosphere in different processing steps, the temperature program, the cooling rate of the glass (especially during fibre drawing) and other factors. For example, a preform and fibre drawn out from it may differ markedly in luminescence properties [10, 11]. When fibres differing in composition are fabricated under similar conditions, it is reasonable to expect that their optical properties are governed by the core composition. It is only in this context that BACs associated with silicon (Si-BACs, responsible for peaks A and B) in the BSG and BGSG fibres or with germanium (Ge-BACs, responsible for peaks D) in the BGSG fibre should be analysed here.

Thus, both the BSG and BGSG fibres have a luminescence peak around 1400 nm (due to Si-BACs in both fibres) and are candidate lasing media. Recent work has demonstrated the feasibility of lasing on the Si-BAC transition responsible for peak A in Fig. 1 [6, 12, 13]. At the same time, our measurements showed that the BGSG fibre had a lower nonselective optical loss level (Fig. 2). More importantly, 1340-nm pumping bleaches the BSG and BGSG fibres: the optical loss drops by about a factor of 60 in the BGSG fibre and by a factor of 7 in the BSG fibre (Fig. 2). This seems to be caused by both germanium doping proper and the lower bismuth content of the BGSG fibre compared to the BSG fibre (as follows from the height of the absorption peaks at 425, 800 and 1410 nm). For this reason, the BGSG fibre (second mode cutoff at 1.2 μm, core–cladding index difference of 7×10^{-3}) was used to make a high-power 1460-nm laser.

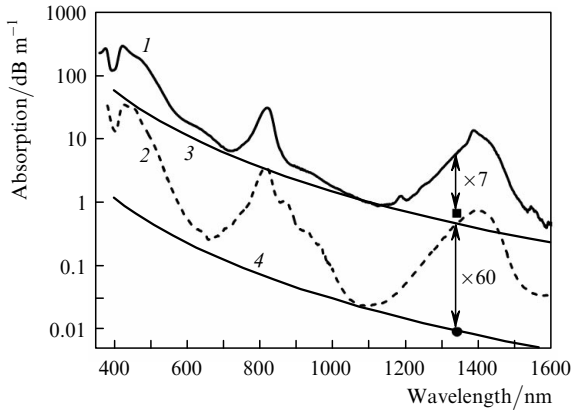

Figure 2. Absorption spectra of the (*1*) BSG and (*2*) BGSG fibres. The points represent the unsaturable optical losses in the fibres at 1340 nm; (*3*, *4*) spectrally nonselective optical loss levels.

The laser configuration is shown in Fig. 3. The bismuth concentration in the fibre core was too low for cladding pumping, so the fibre was core-pumped. The pump source was a single-stage Raman laser operating at 1340 nm, which was, in turn, pumped by an ytterbium fibre laser at 1137 nm. The output power of the Raman laser was 43 W. The cavity of the bismuth fibre laser was formed by a 93-m-long fibre and a Bragg grating with a nearly 100 % peak reflectivity. The cleaved fibre end face served as the output coupler. Figure 4 shows the output power of the bismuth fibre laser as a function of launched pump power. The slope efficiency of the laser is 58 % at pump powers under 15 W. With increasing pump power, the data deviate from linearity, which is probably caused by the heating of the fibre and nonlinear processes (the laser emission bandwidth increased with increasing output power). Nevertheless, the optical efficiency of the bismuth fibre laser was 50 %. Its peak output power was 21.8 W. Note that, in our experiments, no measures were taken to cool the fibre.

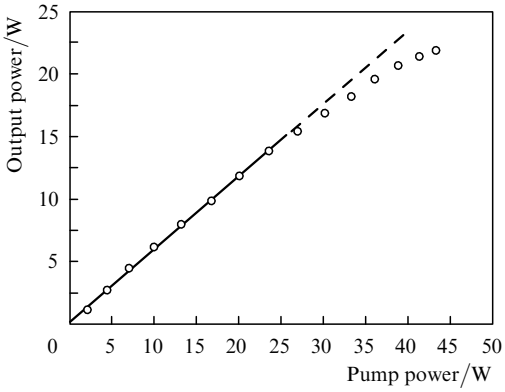

Figure 4. Output power of the bismuth fibre laser at 1460 nm as a function of pump power at 1340 nm.

Thus, the present results indicate that the incorporation of a small amount (~ 5 mol %) of germania into the core of BSG fibre does not break Si-BACs. Germanium doping enables the Si-BACs to be used more effectively (as compared to BSG fibre [6]) for lasing around 1400 nm. We have demonstrated the first efficient bismuth-doped fibre laser operating at 1460 nm with output power above 20 W

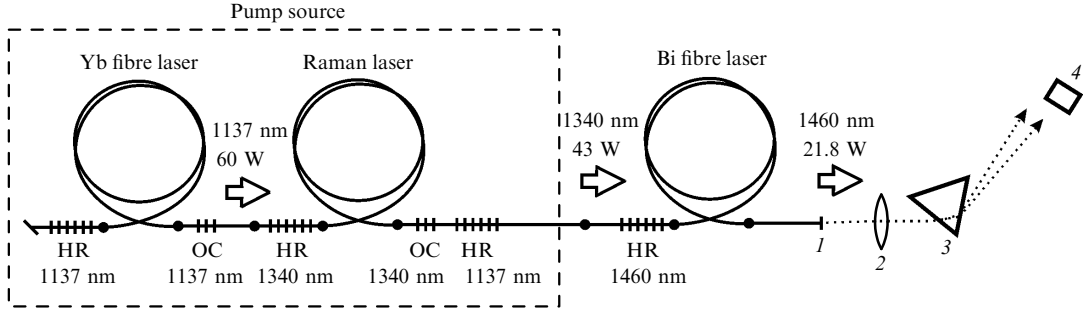

Figure 3. 1460-nm bismuth-doped fibre laser configuration: (*1*) output fibre end, serving as the output coupler; (*2*) collimating objective; (*3*) glass prism; (*4*) power meter; (HR) highly reflective fibre Bragg grating; (OC) output Bragg grating.

and a record optical efficiency (for room-temperature lasing) of 50 %.

References

1. Bufetov I.A., Dianov E.M. *Laser Phys. Lett*., **6**, 487 (2009).
2. Dianov E.M., Shubin A.V., Melkumov M.A., Medvedkov O.I., Bufetov I.A. *J. Opt. Soc. Am. B*, **24**, 1749 (2007).
3. Bufetov I.A., Shubin A.V., Firstov S.V., Melkumov M.A., Khopin V.F., Guryanov A.N., Dianov E.M., in *Proc. CLEO/Europe 2011* (Munchen, 2011) paper CJ8.2 THU.
4. Dianov E.M., Melkumov M.A., Firstov S.V., Shubin A.V., Medvedkov O.I., Bufetov I.A. *Proc. SPIE–Int. Soc. Opt. Eng*., **7580**, 755014-1 (2010).
5. Firstov S.V., Shubin A.V., Khopin V.F., Bufetov I.A., Guryanov A.N., Dianov E.M., in *Proc. CLEO/Europe 2011* (Munchen, 2011) paper PDA7. TUE.
6. Bufetov I.A., Melkumov M.A., Firstov S.V., Shubin A.V., Semenov S.L., Vel'miskin V.V., Levchenko A.E., Firstova E.G., Dianov E.M. *Opt. Lett*., **36**, 166 (2011).
7. Srivastava A.M. *J. Lumin*., **78**, 239 (1998).
8. Gaft M., Reisfeld R., Panczer G., Boulon G., Saraidarov T., Erlish S. *Opt. Mater*., **16**, 279 (2001).
9. Bufetov I.A., Semenov S.L., Vel'miskin V.V., Firstov S.V., Bufetova G.A., Dianov E.M. *Kvantovaya Elektron*., **40**, 639 (2010) [*Quantum Electron*., **40**, 639 (2010)].
10. Razdobreev I., Bigot L., Pureur V., Favre A., Bouwmans G., Douay M. *Appl. Phys. Lett*. **90**, 031103 (2007).
11. Wu J., Chen D., Wu X., Qiu J. *Chin. Opt. Lett*., **9**, 071601 (2011).
12. Dianov E.M., Firstov S.V., Medvedkov O.I., Bufetov I.A., Khopin V.F., Guryanov A.N. *Proc. Conf. OFC-2009* (San Diego, USA, 2009) paper OWT3.
13. Zlenko A.S., Dvoyrin V.V., Mashinsky V.M., Denisov A.N., Iskhakova L.D., Mayorova M.S., Medvedkov O.I., Semenov S.L., Vasiliev S.A., Dianov E.M. *Opt. Lett*., 2011 (to be published).